Multiscale Homogenization Models for the Elastic Behaviour of Metal/Ceramic Composites with Lamellar Domains

Tobias Ziegler[1], Achim Neubrand[1] and Romana Piat[2]

Abstract:

This study predicts the elastic properties of an innovative metal-ceramic composite with statistically oriented domains of parallel ceramic platelets embedded in a eutectic Al-Si-alloy. For this purpose, a two-step homogenisation procedure was employed by finite element- and micromechanical modelling. In a first step, the microstructure of the specimen was divided in domains with the same orientation of lamellae and the elastic properties of single domains were calculated while a precise representation of the shape of the lamellae was attempted. In a second step the elastic characteristics of a large specimen consisting of many domains were computed both by finite element and micromechanical modelling. The experimental Young's modulus of such polydomain specimens was determined by an acoustic resonance method and was lower than predicted. The differences can be explained by microcracks caused by large residual microstresses produced in these materials when they are cooled from the manufacturing temperature.

Keywords: Metal-matrix composites (MMCs) (A); Mechanical properties (B); Finite element analysis (FEA) (C); Modelling (C)

[1] Fraunhofer Institut für Werkstoffmechanik, Wöhlerstraße 11, 79108 Freiburg, Germany, Achim.Neubrand@iwm.fraunhofer.de, +49 761-5142-282, FAX: +49 761-5142-110
[2] Karlsruhe Institute of Technology (KIT), Institute of Engineering Mechanics, Kaiserstraße 12, 76131 Karlsruhe, Germany

1. Introduction

Most crystalline materials exhibit anisotropy at the microscopic scale, and homogenization is necessary to predict the response of large polycrystalline specimens from single crystal data. A common homogenization scheme is the mean-field-approach (MFA) by Hill [1] where the stress and strain fields are averaged over a representative volume element (RVE). Alternatively, a perturbation method can be used to compute the elastic constants of different arrays of rigid spheres in a homogeneous isotropic elastic medium [2]. These methods were compared by Hori and Nemat-Nasser [3]. They found the first order terms in the expanded stress and strain fields to be the same and used this correspondence to formulate a hybrid approach. Counts and co-authors [4] investigated a polycrystalline MgLi alloy and an analytical self-consistency approach as well as finite element modelling (FEM) were employed to obtain the homogenized elastic properties. They favoured the analytical model for its simplicity. There are different micromechanical approximations which can be used for multiphase microstructure modelling. An overview of such methods can be found in monographs by Nemat-Nasser and Hori [5] and Kachanov et al. [6]. A comparison of FEM unit cell models with a Mori-Tanaka MFA was made by Duschlbauer et al. [7] for fibre reinforced composites with a planar random orientation of the fibres. They found an excellent agreement between both methods and concluded that the Mori-Tanaka estimates are fully adequate for predicting the linear responses.

For materials with hierarchical microstructure the multistep homogenization procedure can be used. Such procedures are derived from the Benveniste method [8, 9]. Examples of the application of such methods for different materials can be found for functional graded materials in [10], for polycrystals in [11] and for modelling of the non-elastic repose of the elasto-plastic materials with hierarchical

microstructure in [12, 13]. The general multi-step homogenization method is proposed for shale-type rock materials in [14], for bone in [15] and for rock-like composites in [16, 17].

In this paper we will use such a homogenization procedure for modelling of the microstructure by semi-analytical and FE-methods.

The material under investigation in the present paper is a new type of metal/ceramic composite with a hierarchical structure with randomly orientated regions in one cross section in which all ceramic lamellae are parallel (hitherto called domains, cf. Figure 1 a)). It is produced by infiltrating porous alumina preforms with molten AlSi12 via squeeze-casting. The lamellar microstructure of these preforms is produced by directional solidification along the Z-direction during freezing of a ceramic slurry. The size and internal structure of the domains can be controlled via the freeze casting parameters [18,19]. These lamellar preforms have a high permeability and are thus specifically suited as preform material for the production of metal-ceramic composites via squeeze-casting or even die-casting [20,21] with reinforcement content in the range from 30 to 70 vol.% [22,23]. Due to their elevated ceramic contents such composites are expected to have a high stiffness and wear resistance and are thus of particular interest for applications in the automotive industry.

In a preceding paper, the anisotropic elastic behaviour of single domains in which all lamellae are parallel were investigated by FEM, a micromechanical model and experimentally [24]. In this paper finite element modelling is used to predict the elastic response of a real-world material sample consisting of many domains. The results are compared to micromechanical models established for ideal laminates and composites with ellipsoidal inclusions (Mori-Tanaka and inverse Mori-Tanaka) and to experimental results.

2. Microstructure characterisation and mechanical testing

The processing of the studied AlSi12/Al_2O_3 composites was described in detail earlier [24,25]. The studied materials were produced using melt infiltration of the ceramic preforms, which were produced by freeze-casting at -10°C. The preform architecture is induced through the geometry of the growing ice crystals, and results in a material microstructure with translation symmetry in the direction of ice crystal growth which can be adequately modelled in 2D [26].

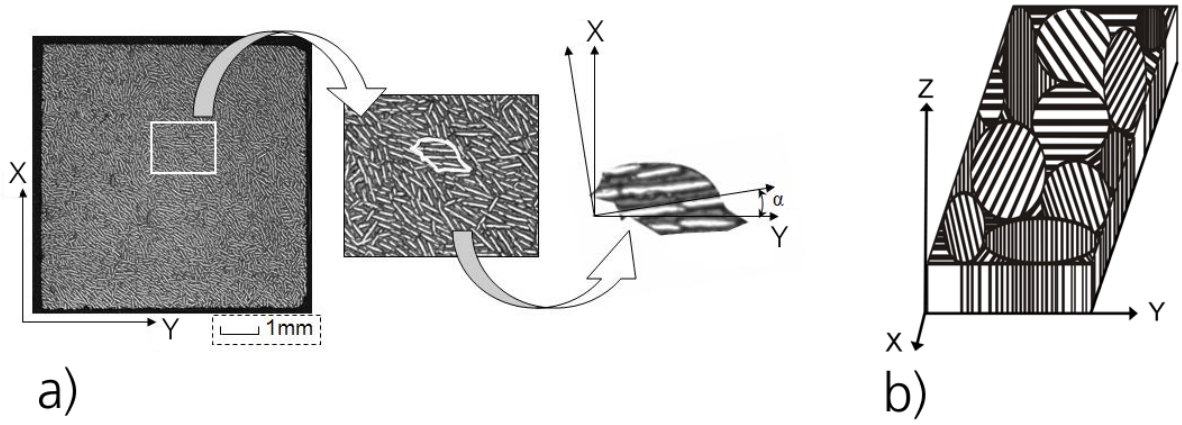

Figure 1**: a)** Polarised light microscopy micrograph of the microstructure and single domain with orientation α to global coordinate system, **b)** Axis convention for a schematic presented polydomain freeze-cast MMC (specimen size 8 x 60 x 40 mm³) used in this study. Z denotes the freezing direction with parallel lamellae; X is the direction of the long side and Y the direction of the short side of the specimen.

The composites under consideration contained between 36 and 42 vol. % of ceramics, which is arranged in domains of parallel lamellae (the ceramic content of the composites was deduced from density measurements of the preform). The typical lamella spacing is about 50 µm (Figure 1 a). Rectangular poly-domain samples with dimensions 8x8x60mm³ were cut from cast blocks of 10x40x60 mm³ size. A

schematic of such a poly-domain sample is shown in Figure 1 b). The edges of the cut poly-domain samples were always parallel to the edges of the original composite plate, i.e. one edge was always parallel to the freezing direction. Mass and dimensions of each sample were measured using a high precision laboratory balance and a micrometer scale, and their densities were determined there from.

The frequency of the first bending resonance was determined for bending in direction Z (axis convention in Figure 1 b). The elastic modulus of these specimens was determined from the weight, the dimensions of the specimen and the resonance frequency according to [27].

3. Modelling

The microstructural modelling of the studied materials was accomplished using two methods: FE-modelling of the real microstructure and micromechanical homogenisation. Both methods use a two step homogenization procedure:

- The polydomain is divided in single domains and the material properties of polydomain (mesoscopic) sample are calculated by averaging over different oriented single domains.
- The anisotropic elastic material parameters of single domains with varying ceramic content are calculated and used as input for the polydomain model.

In the following we show this two-step procedure for FE and micromechanical modelling.

3.1. Finite Element (FE) modelling of the polydomain

For FE-modelling the micrographs of three polydomain specimens with an area of 60 x 40mm² each were used and divided into domains of conform lamella orientation (an example is shown in Figure 2a)). Each domain was then colour-coded with a

colour representing the orientation of the lamellae α in steps of 15°. The resulting domain representation can be seen in Figure 2b).

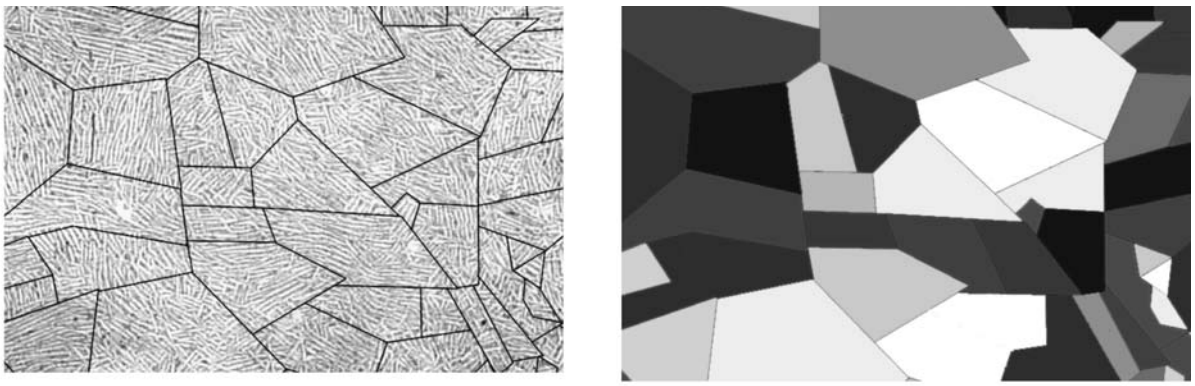

Figure 2: a) Micrograph of a typical polydomain specimen divided into domains of parallel lamellae orientation; b) Each domain was filled with a colour according to the domain orientation angle α.

The different orientation distributions of the domains for three studied microstructures and their average (effective microstructure) in relation to a random domain distribution are presented in Figure 3. For all studied microstructures, some preferred orientations in 30-45° and 90° directions can be observed, but the preference is not very significant (max 8% deviation from random). Insignificance of the influence of such small microstructural variations for the effective material properties of polydomains will be demonstrated later by FEM and micromechanical modelling.

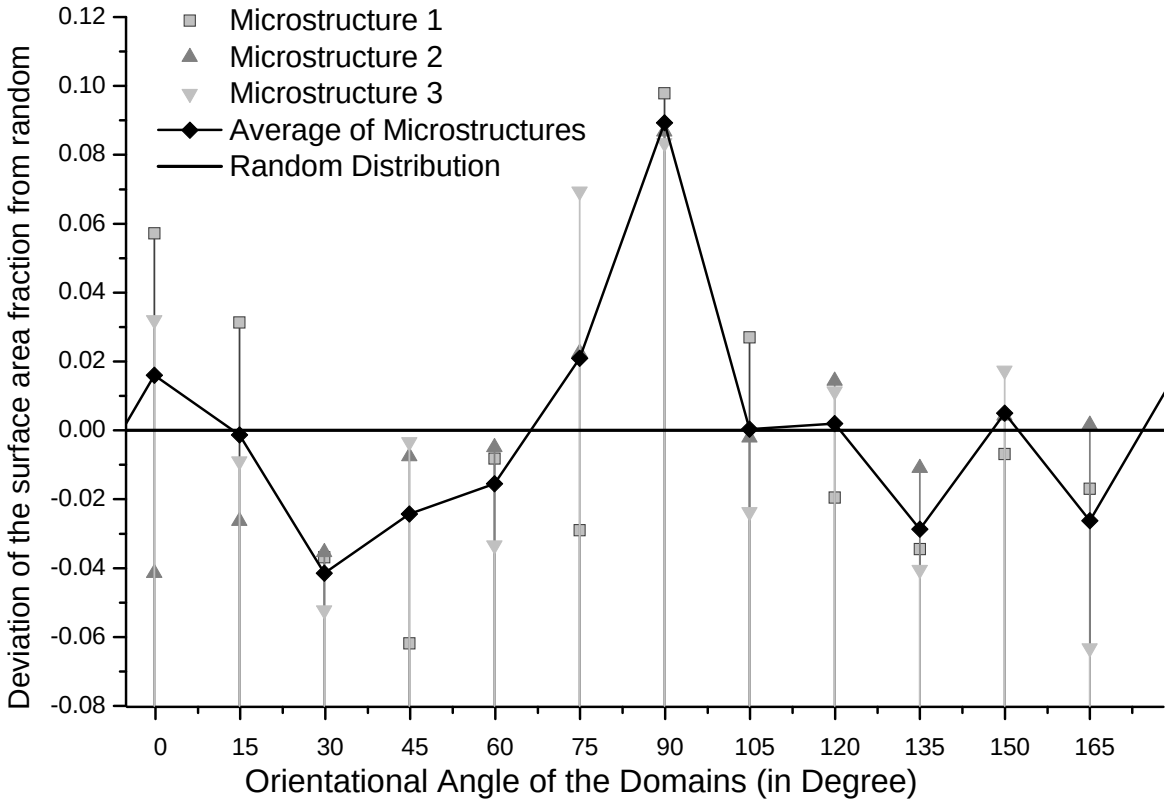

Figure 3: Deviation of the domain distribution from random for three studied microstructures and their average.

The distribution of the lamellae orientation in this material map was used in the FE-model and micromechanical model. The coloured image was imported into the software OOF2® [28] and a FE mesh was adjusted to it where each colour was treated as a different element group. The final mesh was then extruded in the third direction (Z-axis) using Patran® [29] and its elastic behaviour was modelled with the commercially available ABAQUS 6.8 FE-code [30]. In order to determine the unknown components of the stiffness tensor C_{ijkl} of the polydomain, displacements were applied to different sides/faces of the mesh while keeping the nodes on the other sides/faces fixed according to the associated mode of deformation. The components of the stiffness tensor were determined from the resulting stress on the

displaced side for different single domains with varying ceramic contents. In the following we also use the Voigt notation of the stiffness tensors.

3.2. FE-modelling of the single domain

The anisotropic elastic constants for the single domains were taken from the previous modelling of single domain samples with different ceramic contents [24]. Real microstructure FE meshes were generated from microstructure images of entire surfaces of single domain specimens perpendicular to the freezing axis Z (= 1-axis in the single domain model) using the freeware program OOF2 [28]. The 2D-meshes were then extruded along the freezing direction (1-axis) in a subsequent step using Patran (see Figure 4).

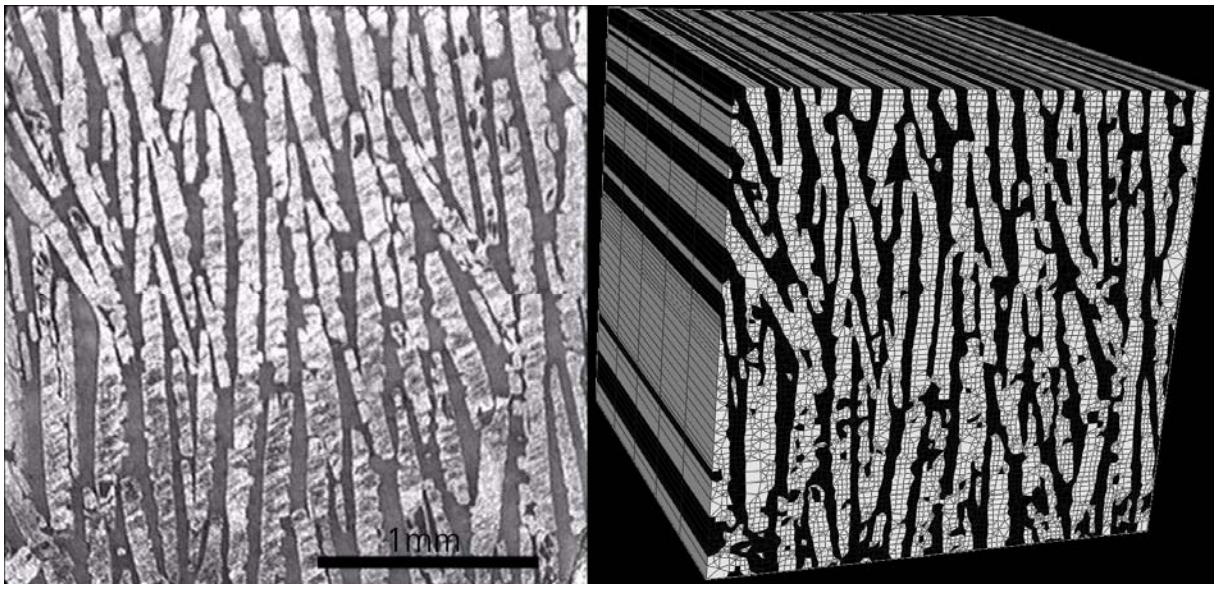

Figure 4: a) Micrograph of a typical single domain specimen viewed from the top (cross section parallel to the freezing direction) b) Real microstructure FE-mesh generated from the micrograph, which were used to compute the elastic constants of single domains.

These meshes were used for obtaining all components of the stiffness tensor assuming an orthotropic symmetry. For alumina an isotropic Young's modulus of 400 GPa and a Poisson's ratio of 0.25 were taken as plausible values from the

literature [31]. For the AlSi12 alloy the Young´s modulus was measured separately to 77.6 GPa, a Poisson's ratio of 0.3 was used for the AlSi12 (for more details we refer to [24]).

3.3. Micromechanical modelling of polydomains

Another possibility for calculation of the effective material properties of the studied materials is micromechanical homogenisation. In our studies we have assumed that the microstructure does not change along the freeze casting direction and the problem can be treated as a 2D-problem.

For micromechanical modelling the same mesoscopic distribution of the different domain orientations as in the FE-model was used (Figure 2 b). For calculation of the effective properties of the microstructure, which consists of differently oriented domains, the following homogenization procedures can be used:

Voigt approximation, which gives stiffer parameters than real ones:

$$\mathbf{C} = \sum_{\alpha=1}^{N} f_\alpha \mathbf{C}^\alpha \; ; \qquad (1)$$

Reuss approximation, which gives the lower bound for material parameters:

$$\mathbf{C}^{-1} = \sum_{\alpha=1}^{N} f_\alpha (\mathbf{C}^\alpha)^{-1} \; . \qquad (2)$$

f_α is the surface fraction of the domains with orientation α and C^α is the stiffness of these domains in the global coordinate system.

For calculation of the effective properties of the polydomain, the stiffness matrix of the single domain C^α is needed.

3.4. Micromechanical modelling of a single domain

For the micromechanical modelling, the Mori-Tanaka and inverse Mori-Tanaka models were applied in which the lamellae (inclusions) with irregular boundaries were approximated as 2D ellipsoids. More about this procedure can be found in [32].

The inverse Mori-Tanaka method gives better estimations than the Mori-Tanaka method for large volume fractions of inclusions (in our case lamellae) and in our case the material had about 58-64 vol. % of inclusions (metal alloy). Mori-Tanaka and inverse Mori-Tanaka correspond to upper and lower estimates for material properties of the domain. In our modelling, we have supposed that the inclusions can be approximated as elliptic cylinders. For this type of inclusions, the components of the Eshelby tensor $\mathbf{S}_c$ can be presented as functions of the half-axes of the ellipses and Poisson ratio of alumina [5, 6].

Then, the Mori-Tanaka model gives the effective stiffness tensor of the domain according to the relation:

$$\mathbf{C}^{dom} = \mathbf{C}^c + f_m(\mathbf{C}^m - \mathbf{C}^c) : \mathbf{A}^m_{(MT)}; \qquad (3)$$

$$\mathbf{A}^m_{(MT)} = [f_m \mathbf{I}^4 + f_c \mathbf{S}_c : (\mathbf{C}^c)^{-1} : (\mathbf{C}^m - \mathbf{C}^c)]^{-1}.$$

Where $\mathbf{I}^4$ is the symmetric fourth-order unit tensor: $I^4_{ijkl} = \frac{1}{2}(\delta_{ik}\delta_{jl} + \delta_{il}\delta_{jk})$; $\mathbf{C}^c$, $\mathbf{C}^m$ and f_c, f_m are stiffness tensors and volume fractions of ceramic and metal phases correspondly.

The stiffness tensor C^α of the single domain with orientation α to global coordinates can be calculated by transformating $\mathbf{C}^{dom}$ into global coordinate system. Inverse Mori-Tanaka model is exactly the same method as Mori-Tanaka, however, the mechanical properties of the matrix and inclusions (i.e. of alumina and aluminium) are permuted.

4. Numerical results

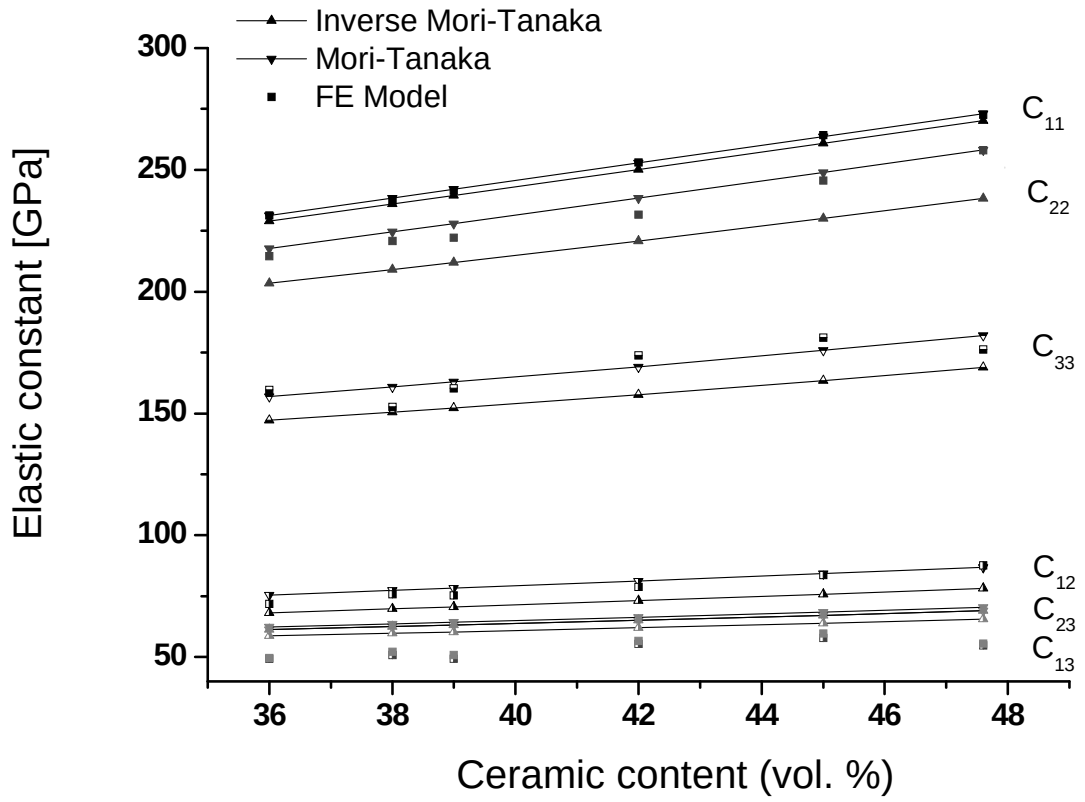

Figure 5: Elastic constants for single domain samples with different ceramic contents. C_{11}, C_{22} and C_{33} are the diagonal elements of the stiffness matrices and C_{12}, C_{13} and C_{23} are the constants for shearing. Results of FEM-calculations and estimations using Mori-Tanaka and inverse Mori-Tanaka models are presented as squares and triangles.

4.1. Elastic properties of single domains

The properties of single domains with parallel lamellae orientation and different ceramic contents were required as input data for the homogenisation. The components of the stiffness tensor, calculated as described in chapters 3.2 and 3.4 using FE and micromechanical modelling are shown in Figure 5. The elastic constants C_{11} along the freezing direction are predicted to be the highest, C_{22} is slightly lower

than C_{11} (around 7% for the FEM), and the lowest values are expected for C_{33} (perpendicular to the lamellae). The calculated shearing constant C_{12} is higher than the other two constants C_{13} and C_{23} which differ only slightly (around 2% for the FEM).

4.2. Elastic properties of polydomains

The elastic constants for large specimens consisting of many domains (as shown in Figure 2) were calculated for different ceramic contents using FE- and micromechanical models. Calculations were carried out in a global coordinate system with direction Z corresponding to the freezing direction (the same as the 1-direction for a single domain). The orientation distribution and corresponding area fractions of the domains were obtained directly from three micrographs as described in 3.1. for both the FE and micromechanical models, while the material properties of single domains were calculated separately. In the micromechanical models, only the results of the inverse Mori-Tanaka model were used for the sequential homogenisation step for the polydomain according to Eqs.(1) and (2). The single domain elastic constants as depicted in Figure 5 were implemented in the FE-model. The results of the different models are shown in Figure 6 for different ceramic contents.

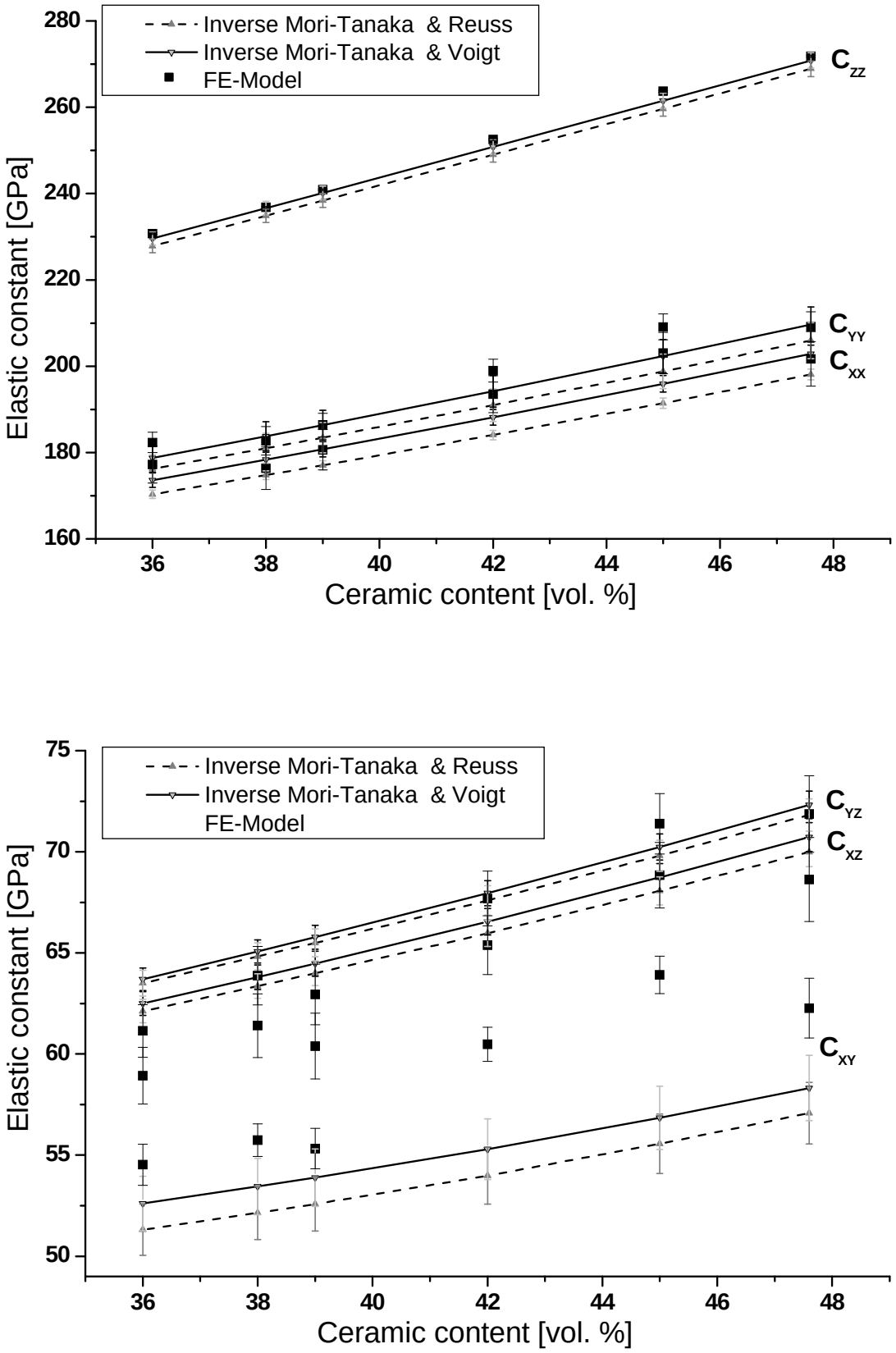

Figure 6: Elastic constants of the mesoscopic models for polydomain specimens. The elastic constants were derived from the single domain elastic constants (FE and inverse Mori-Tanaka

in Figure 5) for six different ceramic contents by inserting those into the FE and micromechanical models. The error bars reflect the microstructural differences of the three analyzed samples.

The constant C_{ZZ} along the freezing direction is the highest for all models. Differences between the three models are small (up to 2%) for this direction. The constants C_{XX} and C_{YY} (perpendicular to the freezing direction) are close but not equal for all three models, and the difference between all models is small. The shearing constants C_{XY}, C_{XZ}, and C_{YZ} differ only slightly with the constant for shearing in the XY-plane being the smallest. All elastic constants increase monotonously with the ceramic content for both models as expected.

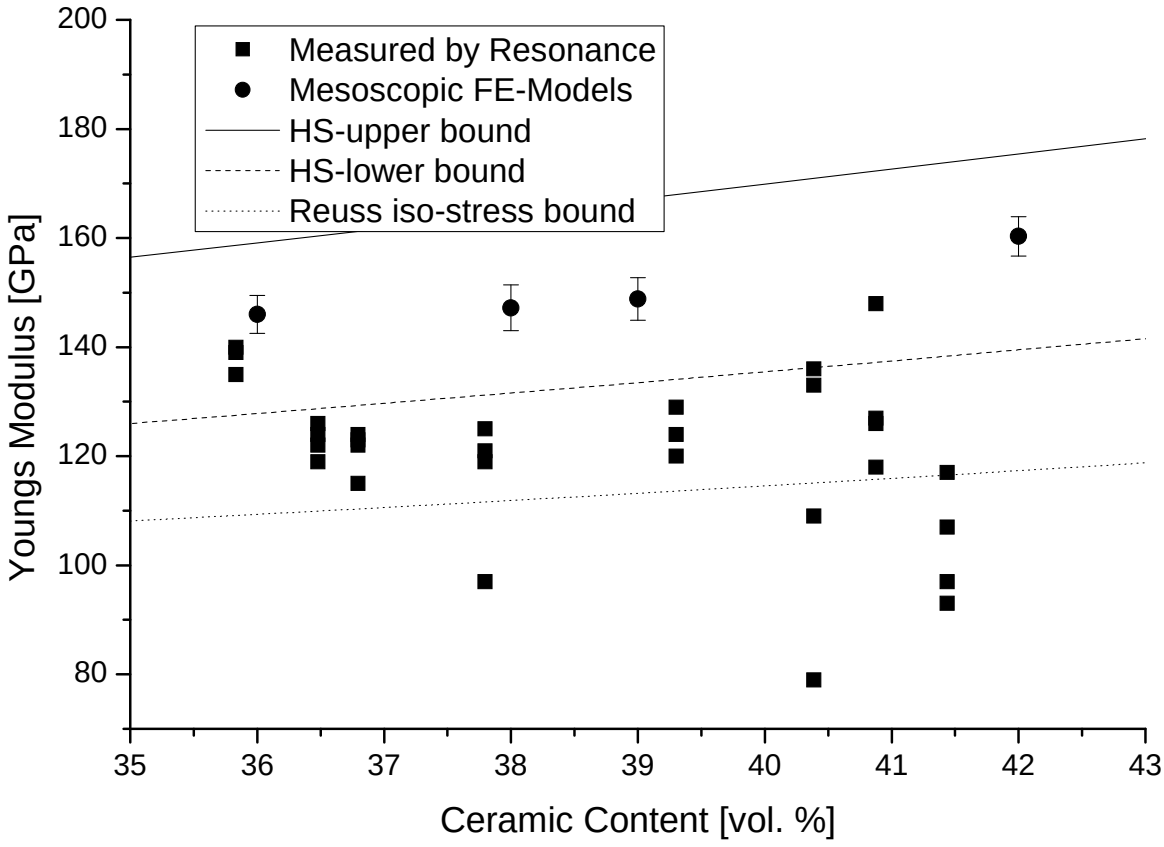

Figure 7: Experimental Young's modulus and FE-modelling data for mesoscopic material are plotted over the ceramic content. The experimental data shows a large scatter. HS-Bounds and the Reuss isostress bound are given for comparison.

The measured Young's modulus in the X-direction of polydomain specimens are compared to the FE-modelling results in Figure 7. The experimental Young's modulus data show a large scatter and are generally lower than the FEM results. No increase with the ceramic content is observable in the experimental results. The upper and lower Hashin-Shtrikman (HS) bounds [33] and the Reuss isostress bound [34] are given for comparison. Most experimental data points are outside of the HS-bounds and some are so low they fall under the Reuss isostress bound. The HS-bounds are given in terms of the bulk and shear moduli as:

$$K^*_{lower} = K_m + \frac{f_c}{\frac{1}{K_c - K_m} + \frac{3 f_m}{3K_m + 4G_m}};$$

$$K^*_{upper} = K_c + \frac{f_m}{\frac{1}{K_m - K_c} + \frac{3 f_c}{3K_c + 4G_c}};$$

$$G^*_{lower} = G_m + \frac{f_c}{\frac{1}{G_c - G_m} + \frac{6(K_m + 2G_m) f_m}{5G_c(3K_m + 4G_m)}};$$

$$G^*_{upper} = G_c + \frac{f_m}{\frac{1}{G_m - G_c} + \frac{6(K_c + 2G_c) f_c}{5G_c(3K_c + 4G_c)}}.$$

where f_m denotes the volume fraction of the metal in the composite and f_c denotes the volume fraction of the ceramic accordingly.

5. Discussion

5.1. Elastic constants of single domains

The FEM and micromechanical results for the single domains in Figure 5 show the highest stiffness along the freezing direction in which a perfectly continuous microstructure is assumed. For a more detailed discussion of the results for normal

modes of deformation and a comparison to experimental data on single domain specimens we refer to [14]. The shearing constants C_{12} are the highest because for this deformation the ceramic lamellae are sheared lengthwise. C_{13} and C_{23} are smaller and have similar values. All constants increase with rising ceramic content of the samples. As real microstructures (an example is depicted in Figure 4) were used for obtaining these results small deviations from a monotonous relationship occur.

5.2. Comparison of micromechanical and FE modelling for polydomains

The mesoscopic FEM and the micromechanical analytical model give very similar results. Correspondence of the constant C_{ZZ} along the freezing in both models is due to identical assumptions being made. Constants C_{XX} and C_{YY} are slightly smaller for micromechanical models compared to the FE-Model (less than 3 GPa). For a perfectly statistical domain orientation C_{XX} and C_{YY} should be identical. In this work, microstructures of real specimens and finite size were analyzed which leads to differences in C_{XX} and C_{YY} from specimen to specimen. For two polydomain specimens C_{YY} was larger than C_{XX} and for one it was vice versa. The deviations of the constants from specimen to specimen are small however and do not indicate a preferential orientation of the domains. Constants C_{XZ} and C_{YZ} calculated using micromechanical models are practically identical for the same volume fractions of ceramic and show good correspondence with values obtained by the FE model. In general, all elastic constants obtained using micromechanical modelling are linear functions of the volume fraction of the ceramic content. Values obtained by FE modelling show a slight nonlinearity.

5.3. Advantages of the FE and micromechanical models

As shown in the last paragraphs, both models can predict the effective properties of the single and polydomains with a high accuracy.

Once implemented, the micromechanical model is fast in calculating the elastic properties of composites and by simple change of the distribution function of the domains it can be applied for estimations for a new microstructure. It can be easily incorporated in other model calculations such as microstructure optimisation, which need fast estimates of the effective properties of variable microstructures.

Such micromechanical estimations were provided for virtual microstructures with random and average domain distributions. Results of these calculations are presented in Figure 8. The difference between Voigt and Reuss bounds for each constant is not significant and has a maximal value of 3% for C_{XX} and C_{YY}. Only the calculations for inverse Mori-Tanaka in combination with Voigt model are presented in Figure 8.

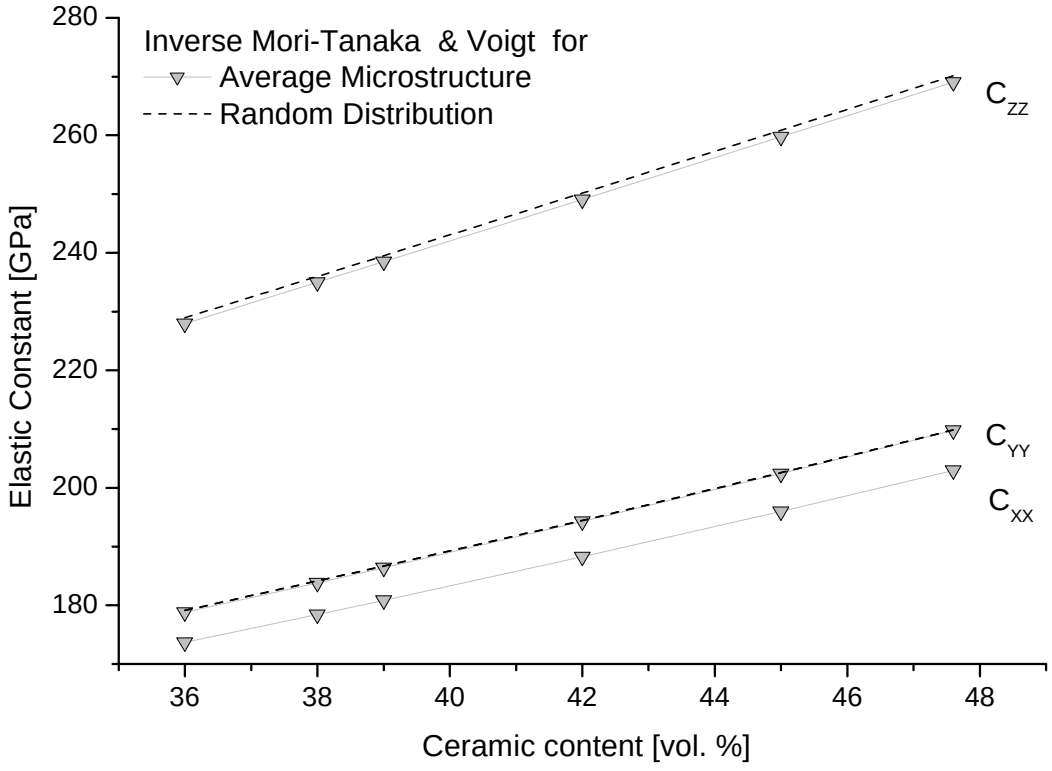

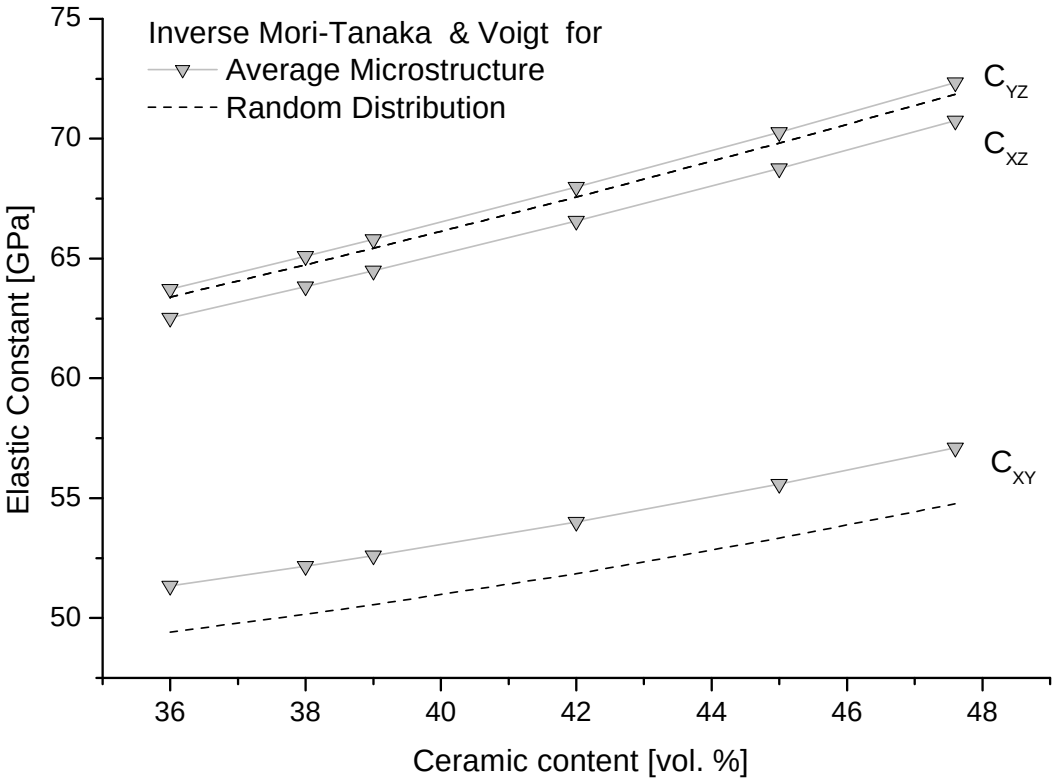

Figure 8: Elastic constants of the virtual microstructures with random and average domain distributions (see Figure 3). Elastic constants for microstructures were calculated using Inverse Mori-Tanaka in combination with Voigt model. The results for random domain distribution are presented as interrupted lines and for the average microstructure as grey lines with triangles.

Analysis of the results shows that for constant C_{zz} there is no difference between the two microstructures. For random domain distribution the constants C_{XX} and C_{YY} as well C_{XZ} and C_{YZ} are identical, therefore only one interrupted line is visible. The difference between both microstructures becomes apparent at the constants C_{XX} and C_{YY}, which differ by up to 7 GPa. The constants C_{XY} are larger for the average distribution and the maximal difference as compared to the random distribution is 3 GPa.

Finite element modelling requires more effort as compared to the analytical model, but allows a better insight into the stress and strain distributions within the

microstructure. An example is shown in Figure 9. It can be seen that domains with lamellae oriented along the loading direction show high tensile stresses (solid white arrows) and that domains perpendicular to the loading direction show lower tensile or even compressive stresses (dotted white arrows). This stress distribution is advantageous, because experiments on small single domain samples showed that the strength is highest along this direction. The FEM model can be extended to include plasticity and account for the thermal residual stresses that result from the infiltration process.

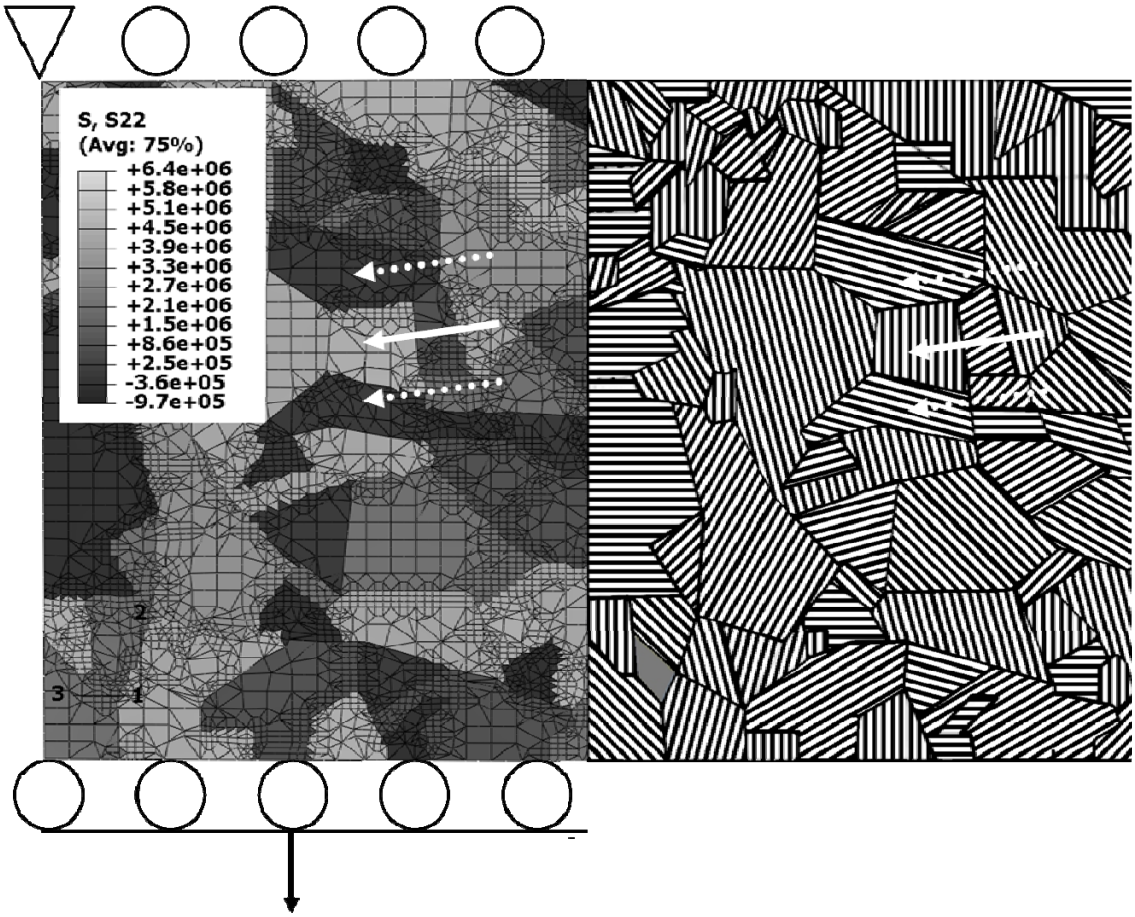

Figure 9: left: Detail of the σ_{22} (in Pa) stress distribution in the microstructure for a vertical load (along the 2-direction) in the mesoscopic model for 39 % ceramic content. Right: shape and orientation of the domains in the polydomain specimen modelled on the left. The solid white arrows indicate a domain with high stresses and lamellae oriented along the loading

direction while the dotted white arrows point to domains with low stresses and lamellae oriented perpendicular to the load.

5.4. Comparison of modelling results with experimental values

Figure 7 shows a discrepancy between experimental and modelling results for the elastic modulus. This could be due to the resonance method not taking the anisotropy of the material into account. Calculation of the resonance modes on the 3D FE-model showed only a minor influence (less than 1%) of the occurring anisotropy on the resonance frequency of the material. Hence, errors in experimental methodology can be excluded as a reason for the discrepancy. Nevertheless, the experimental values are typically considerably lower than predicted by the FE-and HS models. This indicates that the assumptions made in these models (dense material, no microcracks or debonded interfaces) do not apply to the material as produced. Indeed, radiographic images of most composite specimens show some residual porosity (areas which are not completely infiltrated with metal). Density measurements indicate that this porosity cannot be very large (less than 3% on average). Both, estimates using microstructural models and our previous experience with infiltrated MMC indicate that this porosity could only account for a moderate modulus reduction of less than 10 GPa as compared to a dense specimen. However, radiographic images of some specimens showed cracks perpendicular to the image plane that were large enough to be visible. As the metal-ceramic-interfaces of the lamellar specimens lie in this plane it is very likely that the cracks run along or very near this interface. We believe that the aforementioned relatively large cracks can best account for the very low modulus observed in some specimens and its large scatter. We believe that these cracks may have formed during cooling from the

infiltration temperature at the interfaces between domains of different lamella orientation. Elastoplastic FE calculations show a very strong anisotropy of thermal contraction, which can differ by a factor of more than three for different lamella orientations. Elastoplastic modelling of polydomain specimens shows high thermal residual stresses at domain interfaces which could well account for the observed crack formation.

6. Conclusion

The elastic constants of a novel MMC microstructure consisting of domains with parallel ceramic lamellae could be predicted with multiscale FE and micromechanical models. The FE model was based on the real microstructure and represented the irregular shape of the ceramic lamellae on the microscale whereas the micromechanical model was based on the Mori-Tanaka approach and approximated the lamellae as 2D ellipsoids. The results achieved with the two approaches are similar and the largest differences in predicted elastic constants of a polydomain specimen were only a few GPa. Both models have their advantages. The micromechanical model is easily applicable for different microstructures and could be used as a step for more complicated calculations. The FE model was able to reveal large differences in the stress state of different domains under external tensile loading - the largest stresses occurred in domains with lamella orientation parallel to the applied stress.

Acknowledgements

We thank A. Wanner and S. Roy of the Institut für Werkstoffkunde, University of Karlsruhe for providing micrographs of single domain specimens, and M.J. Hoffmann, R. Oberacker, and T. Waschkies of the Institute for Ceramics in Mechanical

Engineering, University of Karlsruhe, as well as A. Nagel and O. Lott, Faculty of mechanical engineering / materials science at Aalen University, Aalen, Germany, for providing the specimen material. Financial support from Deutsche Forschungsgemeinschaft (DFG), Bonn, Germany under projects Ne599/6-1 and PI785/1-1 is gratefully acknowledged.

---

[1] Hill, R., Elastic properties of reinforced solids: some theoretical principles, Journal of the Mechanics and Physics of Solids, 1963;11:357–372.

[2] Nunan, K. & Keller, J., Effective elasticity tensor of a periodic composite, Journal of the Mechanics and Physics of Solids 1984;32:259–280.

[3] Hori, M. & Nemat-Nasser, S., On two micromechanics theories for determining micro-macro relations in heterogeneous solids, Mechanics of Materials 1999;31:667–682.

[4] Counts, W., Friák, M., Battaile, C. & Raabe, D., A comparison of polycrystalline elastic properties computed by analytic homogenization schemes and FEM, phys. stat. sol.(b) 2008;245(12), 2630–2635.

[5] Nemat-Nasser S., Hori M.: Micromechanics: overall properties of heterogeneous materials (Elsevier, Holland1999).

[6] M. Kachanov, B. Shafiro, I.Tsukrov, Handbook of elasticity solutions. Kluwer academic publishers, 2004.

[7] Duschlbauer, D. Böhm, H.J. Pettermann, H.E., Computational simulation of Composites Reinforced by Planar Random Fibers: Homogenization and Localization by Unit Cell and Mean Field Approaches, Journal of Composite Materials 2005;40:2217-2234

[8] Benveniste, Y., A new approach to the application of Mori–Tanaka's theory in composite materials. Mechanics of Materials 1987; 6: 147–157.

[9] Benveniste, Y., Dvorak, G.J., Chen, T., Stress fields in composites with coated inclusions. Mechanics of Materials 1989; 7(4): 305–317.

[10] Genin G. M., Birman V., Micromechanics and structural response of functionally graded, particulate-matrix, fiber-reinforced composites, International Journal of Solids and Structures 2009; 46: 2136-2150

[11] Iwakuma T., Koyama S., An estimate of average elastic moduli of composites and polycrystals. Mechanics of Materials 2005; 37: 459-472.

[12] Doghri I., Tinel L., Micromechanical modelling and computation of elasto-plastic materials reinforced with distributed-orientation fibers, International Journal of Plasticity 2005; 21:1919–1940.

[13] Friebel C., Doghri I., Legat V., General mean-field homogenization schemes for viscoelastic composites containing multiple phases of coated inclusions, International Journal of Solids and Structures 2006; 43: 2513–2541.

[14] Ulm, F.J., Delafargue, A., Constantinides, G., 2005. Experimental microporomechanics. In: Dormieux, L., Ulm, J.F. (Eds.), Applied Micromechanics of Porous Materials. Springer.

[15] Hellmich Ch., 2005. Microelasticity of bone. In: Dormieux, L., Ulm, J.F. (Eds.), Applied Micromechanics of Porous Materials. Springer.

[16] Giraud A., Huynh Q.V., Hoxha D., Kondo D., Application of results on Eshelby tensor to the determination of effective poroelastic properties of anisotropic rocks-like composites. International Journal of Solids and Structures 2007; 44 (11–12): 3756–3772.

[17] Giraud A., Huynh Q.V., Hoxha D., Kondo D. , Effective poroelastic properties of transversely isotropic rock-like composites with arbitrarily oriented ellipsoidal inclusions, Mechanics of Materials 2007; 39: 1006–1024.

[18] Waschkies, T. Oberacker, R. Hoffmann, M.J.: "Tailor-Made Ceramic Preforms by Freeze-Casting", 10th International Conference on Ceramic Processing Science, Japan, May 25-28, 2008, to be published in the Journal of American ceramic Society, Januray 2009

[19] Fukasawa T, Ando M, Ohji T, Kanzaki S. Synthesis of porous ceramics with complex pore structure by freeze-dry processing. J. Am. Ceram. Soc. 2001; 84(1): 230-232

[20] Ghomashchi MR, Vikhrov A. Squeeze casting: an overview. J. Mater. Process. Technol. 2000; 101: 1-9

[21] Clyne TW, Mason JF. The squeeze infiltration process for fabrication of metal-matrix composites. Metall. Trans. A 1987; 18A: 1519-1530

[22] Deville S, Saiz E, Nalla RK, Tomsia AP. Freezing as a part to build complex composites. Science 2006; 311: 515-518

[23] Deville S, Saiz E, Tomsia AP. Ice-templated porous alumina structures. Acta Mater. 2007; 55: 1965-1974

[24] Ziegler, T. Neubrand, A. Roy, S. Wanner, A. Piat, R., Elastic constants of metal/ceramic composites with lamellar microstructures: Finite element modelling and ultrasonic experiments. Composites Science and Technology 2009;69(5):620-626

[25] Waschkies T, Oberacker R, Hoffmann MJ, Control of lamellae spacing during freeze casting of ceramics using double-sided cooling as a novel processing route, J. A. Ceram. Soc. 92 [S1] S79–S84 (2009)

[26] S. Roy and A. Wanner, Metal/Ceramic Composites from Freeze-Cast Ceramic Preforms: Domain Structure and Elastic Properties, Compos. Sci. Technol. 2008; 68: 1136–43.

[27] ASTM International (American Society for Testing and Materials) C1259-94

[28] OOF2: Object-Oriented Finite Element Analysis of Material Microstructures developed by Steve Langer, Andrew Reid, Rhonald C. Lua, Valerie R. Coffman, R. Edwin Garcia and Ed Fuller, National Institute of Standards and Technology, Gaithersburg, US

[29] Patran MSC Software, Santa Ana, CA, USA

[30] ABAQUS, Simulia, Providence, RI, USA

[31] National Institute of Standards and Technology, Property Data Summary: http://www.ceramics.nist.gov/srd/summary/Al2O3.htm

[32] Piat R., Tsukrov I., Mladenov. N., Guellali M., Ermel R., Beck T., Schnack E., Hoffmann M. J.: Material modelling of the CVI-infiltrated C-felt. II. Statistical study of the microstructure, numerical analysis and experimental validation. Compos. Sci. Technol. 2006; 66(15): 2769-2775.

[33] Hashin, Z. & Shtrikman, S., 'A variational approach to the theory of the elastic behaviour of multiphase materials', Journal of the Mechanics and Physics of Solids 1963;11: 127–140.

[34] Reuss A., Berechnung der Fließgrenze von Mischkristallen auf Grund der Plastizitätsbedingung für Einkristalle, Z. Angew. Math. Mech. 1929; 9:49 - 58